

See discussions, stats, and author profiles for this publication at: <https://www.researchgate.net/publication/231654293>

Mobility of n-butane in ZSM-5 zeolite studied by ^2H NMR

ARTICLE in THE JOURNAL OF PHYSICAL CHEMISTRY C · FEBRUARY 2010

Impact Factor: 4.77 · DOI: 10.1021/jp908464f

CITATIONS

7

READS

26

3 AUTHORS, INCLUDING:



Daniil Kolokolov

Boreskov Institute of Catalysis

28 PUBLICATIONS 305 CITATIONS

SEE PROFILE



Alexander G Stepanov

Boreskov Institute of Catalysis

136 PUBLICATIONS 1,679 CITATIONS

SEE PROFILE

Mobility of *n*-Butane in ZSM-5 Zeolite Studied by ^2H NMRDaniil I. Kolokolov,^{†,‡} Hervé Jobic,[‡] and Alexander G. Stepanov^{*,†}

Boreskov Institute of Catalysis, Siberian Branch of Russian Academy of Sciences, Prospekt Akademika Lavrentieva 5, Novosibirsk 630090, Russia, and Institut de Recherches sur la Catalyse et l'Environnement de LYON, CNRS, Université de Lyon, 2 av. Albert Einstein, 69626 Villeurbanne, France

Received: September 2, 2009; Revised Manuscript Received: January 19, 2010

The mobility of linear alkane, *n*-butane, adsorbed in zeolite ZSM-5 was investigated by deuterium solid-state NMR (^2H NMR). Analysis of the ^2H NMR spectra line shape and spin–lattice relaxation time permitted characterizing the influence of pore confinement on the dynamics of the molecule over a broad temperature range (123–413 K). It has been found, that at a loading of two molecules per unit cell, *n*-butane molecules are essentially located in both straight and zigzag channels and not the intersections. The adsorbed molecules are involved in fast intramolecular motions and reorientation as a whole. Intramolecular motions are methyl group rotation and conformational exchange occurring at $\tau \approx 4\text{--}8 \times 10^{-11}$ s (at 300 K) with an activation barrier of $E_{\text{ci}} \approx 11\text{--}12$ kJ mol $^{-1}$. The reorientation of the molecule as whole is a complex anisotropic motion, which consists of jump exchange between neighboring channels, occurring at $\tau_{\text{D}} \approx 3.7 \times 10^{-10}$ s (at 300 K) with an activation barrier of $E_{\text{D}} \approx 5$ kJ mol $^{-1}$ and of other rotational modes that may correspond to uniaxial rotation and librations of *n*-butane in the pores. Influence of pore confinement on the dynamics of the adsorbed alkane is manifested by the complete suppression of isotropic reorientation.

1. Introduction

Zeolites, in particular the ZSM-5 type, are widely used in industry in such important processes as fluid catalytic cracking, oil refining,^{1,2} and hydrocarbons separation.^{3,4} In all these processes the key factor is the unique shape-selectivity of the zeolite.⁵ The shape-selectivity is a result of how the guest molecules interact with the host matrix under conditions, when the size of the guest and the pore are commensurable.⁶ The understanding of such pore confinement phenomenon should give clear indications of what to expect from a zeolite/sorbate system and of directions in which the host matrix should be modified in order to achieve better performance.

Because of its practical and fundamental interest over past years, the interaction of guest molecules with the host-matrix was intensely elaborated both experimentally and by simulation. Practically, a large number of both theoretical and experimental studies were focused on sorption and thermodynamic properties of different guest molecules (mainly hydrocarbons), and considerable progress was actually achieved.⁷ However, regarding the microscopic dynamics of guest molecules in tight confinement much is still not understood.

Experimentally the microscopic dynamics of molecules trapped in zeolite micropores can be accessed only by several techniques. These are pulsed field-gradient NMR (PFG-NMR)⁴ and quasi-elastic neutron scattering (QENS)⁸ or neutron spin–echo technique⁹ to measure the translational diffusion. As to the rotational motion, different solid-state NMR techniques (1D or 2D: ^{13}C , ^2H)¹⁰ or again neutron scattering methods can be used.

Molecular simulations allow a deeper understanding of the experimental results. Various simulation techniques, especially molecular dynamics (MD) proved to be quite efficient to predict

thermodynamics and sorption properties for a number of guest molecules in different zeolite structures.^{11,12} However, this is still not the case for transport/mobility properties of adsorbed species.⁷ On one hand the present discrepancies can be explained by computation difficulties: the computation of MD for long hydrocarbons in a zeolite is a resource-demanding procedure, and usually the simplified representations of adsorbates are used. But it is clear, that in such a tight confinement, rotational degrees of freedom of the sorbate can strongly affect the transport diffusivity and therefore should accurately be taken into account. It was demonstrated by Theodorou et al.¹³ that already in the case of *n*-butane the conformational exchange plays an important role in the mechanism of translational jump diffusion. On the other hand, direct experimental data on rotational dynamics for a chosen hydrocarbon is not always available, for instance, for *n*-butane only QENS¹⁴ and PFG NMR¹⁵ diffusivity studies were performed.

In such context the elucidation of the rotational dynamics of the *n*-butane in ZSM-5 pores is of a special interest. Such system is of a great applied interest, and it is still not too complex to be accessible for simulations. So it is an good candidate for detailed comparison between experimental and theoretical studies. Such comparison should bring to a more adequate approximation of the effective potential¹¹ used for theoretical description of the interaction of linear alkanes with zeolite ZSM-5 walls. The potential of a tight combination of experimental and simulation study of dynamics in a similar system, pentane in KFI zeolite, was recently shown.^{16,17}

Lastly, from physical point of view, the mobility in zeolites represents a particular case of dynamics, placed between solids on one side and liquids or gases on the other one. As in solids, adsorbed species suffer heavy restrictions in their motion, and certain modes can be dumped or even completely inaccessible (e.g., free rotational diffusion), but at the same time, the remaining modes are well pronounced and show characteristic times usual for a liquid state.

* To whom correspondence should be addressed. Phone: +7 383 326 9437. Fax: +7 383 330 8056. E-mail: stepanov@catalysis.ru.

[†] Siberian Branch of Russian Academy of Sciences.

[‡] Université de Lyon.

In this work we present the experimental solid state ^2H NMR study of the *n*-butane dynamics inside the ZSM-5 zeolite pores at low loadings (to avoid intermolecular interactions). ^2H NMR has been shown to be a powerful tool to probe the dynamics of molecular species confined in microporous materials.^{18–24} The spectrum line shape and spin relaxation of ^2H nuclei is mainly governed by electric intramolecular quadrupolar interaction,^{25,26} which gives the possibility to characterize the molecular dynamics over a broad time scale from 10^{-4} – 10^{-6} s to 10^{-8} – 10^{-10} s, respectively.

2. Experimental Section

2.1. Materials. A H-ZSM-5 sample with Si/Al ratio of 58 was prepared from Na-ZSM-5 via NH_4 ion exchange and subsequent calcination at 820 K as described.²⁷ The obtained zeolite sample was characterized by X-ray powder diffraction and chemical analysis. Perdeuterated *n*-butane- d_{10} with 98% ^2H isotopic enrichment was purchased from Cambridge Isotope Laboratories, Inc. and was used without further purification.

2.2. Samples Preparation. To prepare samples for the NMR experiments, approximately 0.3 g of H-ZSM-5 zeolite was loaded in a 5 mm (outside diameter) glass tube, connected to a vacuum system. The sample was then heated at 670 K for 2 h in air and for 24 h under vacuum of 10^{-5} Torr (1 Torr = 133.3 Pa). After the sample was cooled back to room temperature, the zeolite was loaded with certain amount of *n*-butane and sealed off. The loading was ~ 2 molecules per unit cell of the zeolite. The adsorption was performed from the gas phase with the zeolite powder kept at the temperature of liquid nitrogen. The sealed sample was finally heated for 10 h at 373 K to obtain a uniform distribution of the adsorbed *n*-butane over the zeolite sample. No quantity of *n*-butane was detected on outer surface of the zeolite samples after long time heating at 373 K, as it followed from analysis of the ^2H NMR line shapes.

2.3. NMR Measurements. ^2H NMR experiments were performed at 61.432 MHz on a Bruker Avance-400 spectrometer, using a high power probe with 5 mm horizontal solenoid coil. All ^2H NMR spectra were obtained by Fourier transformation of the quadrature detected quadrupole echo, arising in a pulse sequence^{28,29}

$$\left(\frac{\pi}{2}\right)_{\pm X} - \tau_1 - \left(\frac{\pi}{2}\right)_Y - \tau_2 - \text{acquisition} - t \quad (\text{i})$$

where $\tau_1 = 30 \mu\text{s}$, $\tau_2 = 34 \mu\text{s}$, and t is a repetition time for the sequence (i) during the accumulation of NMR signal. The duration of the $\pi/2$ pulses was 3.0–4.5 μs . Spectra were typically obtained with 500–5000 scans and a repetition time $t = 1$ –2 s. Inversion–recovery experiments, to derive spin–lattice relaxation times (T_1), were carried out using the pulse sequence:³⁰

$$(\pi)_X - t_v - \left(\frac{\pi}{2}\right)_{\pm X} - \tau_1 - \left(\frac{\pi}{2}\right)_Y - \tau_2 - \text{acquisition} - t \quad (\text{ii})$$

where t_v was a variable delay between the 180° $(\pi)_X$ inverting pulse (as in standard inversion–recovery pulse sequence³⁰) and the quadrupole echo sequence (i). T_1 values for overlapping signals from CD_3 and CD_2 groups were calculated on the basis of the time ($\tau_0 = 0.693 T_1$).³⁰ τ_0 is the time t_v for which the intensity of the NMR line changes from the inverted negative position to the normal positive one in the inversion–recovery

experiment (sequence (ii)). T_1 values were measured with accuracy of 20%: the overlapping signal from CD_2 and CD_3 groups in a part of the experimental temperature range had similar relaxation time values, which complicated the analysis of the raw data. It should be mentioned that at each temperature we have measured both the zero crossing and the full recovery curve, especially to check its homogeneity. In each case, the recovery curve showed a monoexponential dependence within the accuracy level.

The temperature of the samples was controlled with a flow of nitrogen gas, stabilized with a variable-temperature unit (Bruker model BVT-3000) with a precision of ~ 1 K; the sample was allowed to equilibrate at least 15 min at a given temperature before the NMR signal was acquired.

2.4. Data Treatment. The NMR data acquisition and treatment was performed using BRUKER TopSpin commercial software. All simulations and fitting procedures were performed using homemade FORTRAN routines according to the formalism described in refs.^{31,32}

3. Results and Discussion

3.1. ^2H NMR Spectra of Adsorbed Deuterated *n*-Butane- d_{10} . To study the dynamics of adsorbed *n*-butane- d_{10} ^2H NMR spectra were recorded in a temperature range of 123–413 K. The experimental results are presented in column a of Figure 1 together with simulated ones (column b). ^2H NMR line shape reflects the way of the C–D bonds reorientation in *n*-butane- d_{10} , while the molecule is exploring the zeolite pores. In *n*-butane, there are two types of nonequivalent C–D bonds with regard to their motional behavior, i.e., the CD_2 and the CD_3 groups (see Figure 2). So the total line shape is a sum of signals from CD_3 and CD_2 groups, i.e., each simulated spectrum is a superposition of two line shapes with effective parameters Q_{eff} and η (Figures 2 and 3). Decomposition of the spectrum into two signals requires a certain justification. In fact, the validity of such an assumption is clear and straightforward only when there is a fast ($\tau_C \ll 1/Q_0 \approx 10^{-6}$ s) exchange between all possible positions of the adsorbed *n*-butane. In other words, all motions in which CD_3 and CD_2 groups of adsorbed *n*-butane are involved, are found in the fast limit regime ($\tau_C \ll 1/Q_0$). There are direct experimental observations to support this hypothesis. QENS measurements reported by Jobic et al.¹⁴ show that *n*-butane adsorbed in ZSM5 is involved into translational jump diffusion (see Table 1). The residence time of the translational diffusion is characterized by an activation barrier of $E_D = 5 \text{ kJ mol}^{-1}$ and a pre-exponential factor $\tau_{D0} = 2 \times 10^{-11}$ s. In addition to the translational diffusion, QENS data points to the presence of the uniaxial rotation of *n*-butane molecules in the zeolite channels: the average characteristic time of this process $\tau_R \approx 1.5 \times 10^{-11}$ s and the temperature dependence is so weak that only the estimation of the upper threshold for the activation energy is possible, so $E_R < 4 \text{ kJ mol}^{-1}$. These two characteristic times prove, that even at $T \approx 100 \text{ K}$, *n*-butane is involved into fast on the ^2H NMR time scale ($\tau_D \ll 1/Q_0 \sim 10^{-6}$ s) translational diffusion and an even faster uniaxial rotation. Moreover, in addition to QENS measurements, the characteristic times of rotational motions in *n*-butane can be estimated directly from the spin–lattice relaxation time temperature dependence (vide infra). It follows from relaxation measurements that even at lowest temperatures the characteristic times are smaller than 10^{-7} s. This supports our assumption that all relevant motions in the system are found in the fast limit regime on the ^2H NMR time scale.

The spin–lattice relaxation offers an additional possibility to check the spectrum composition. It follows from the T_1

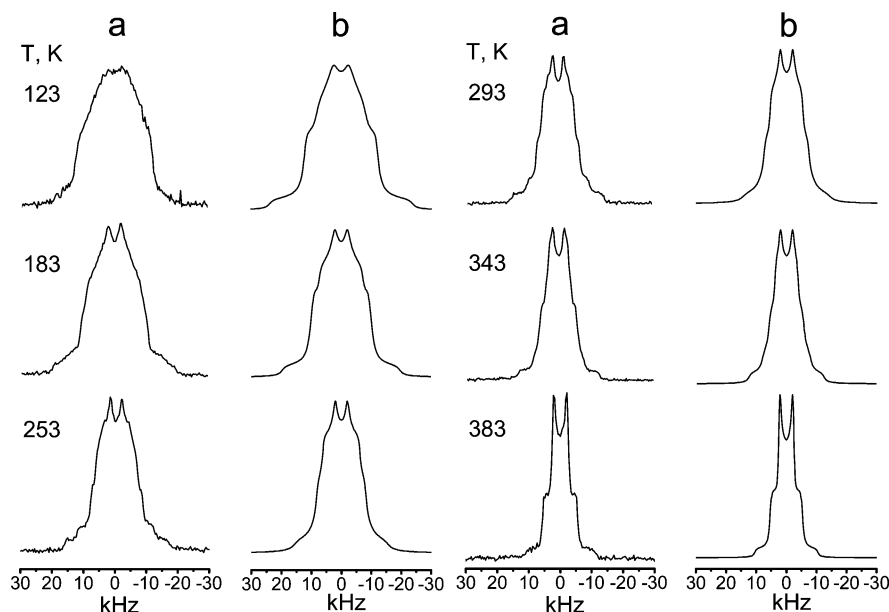


Figure 1. Temperature dependence of ^2H NMR line shape of n -butane- d_{10} adsorbed on H-ZSM-5 zeolite: experimental (a) and simulated (b) spectra.

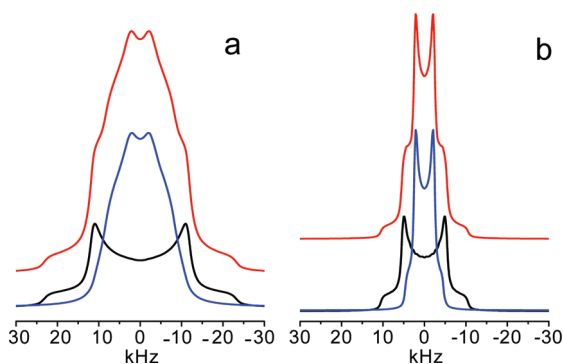


Figure 2. The ^2H NMR spectra of n -butane- d_{10} is a sum of signals from CD_2 and CD_3 deuterons. An example is provided for two distinct temperatures: 143 K (a) and 383 K (b). The CD_2 groups signal is shown in black, the CD_3 in blue, and the their sum in red.

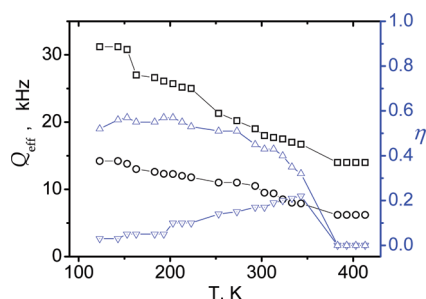


Figure 3. Temperature dependence of the effective Q_{eff} and η parameters for n -butane- d_{10} adsorbed on H-ZSM-5 zeolite. CD_2 group: Q_{eff} (\square) and η (∇); CD_3 group: Q_{eff} (\circ) and η (\triangle).

temperature dependence that the signals from CD_3 and CD_2 groups have notably different spin–lattice relaxation times above ~ 203 K, so the inversion–recovery pulse sequence can be used as a filter and a separate observation of both signals can be performed.³⁸ All the arguments given above prove that the decomposition of the spectrum in two signals reflects the actual physical picture and the all motions are fast enough.

The change of the line shape from both CD_2 and CD_3 groups with temperature reflects the evolution of motions in which these two molecular fragments are involved. Technical details of the

TABLE 1: Parameters of the Translational Jump Diffusion of n -Butane- d_{10} Adsorbed on H-ZSM-5 Zeolite Measured by QENS¹⁴

	300 K	353 K	413 K
D , $\text{m}^2 \text{s}^{-1}$	1×10^{-9}	1.4×10^{-9}	1.8×10^{-9}
τ_D , s	1.4×10^{-10}	1.17×10^{-10}	9×10^{-11}
$l_0 = \langle l^2 \rangle^{1/2}$, nm	0.92	0.99	0.99

effect of the molecular motion on ^2H NMR line shape were already discussed in a vast number of papers and can be found elsewhere.^{26,31,33–36} In short, any fast enough molecular motion in which the n -butane molecule is involved averages in some certain way the initial static ^2H NMR spectrum, a Pake-powder doublet, characterized by a quadrupolar constant $Q_0 \sim 170$ kHz and asymmetry parameter $\eta \approx 0$.³³ The signal from the CD_3 group of the adsorbed n -butane- d_{10} should give a line shape with smaller effective Q_{eff} than that from the CD_2 , since the methyl groups are additionally involved in a three site jump rotation around the C- CD_3 bond. This allows us to discuss only the mobility the CD_2 group since the analysis for the CD_3 should be straightforward.

As it was already discussed, the experiments show, that n -butane is highly mobile even at lowest temperature probed (123 K) and the quadrupole constant is already strongly averaged, $Q_{\text{eff}}^{\text{CD}_2} \approx 31$ kHz (in the absence of any motion the $Q_0 \approx 170$ kHz). On the other hand, even at highest temperature (413 K) $Q_{\text{eff}}^{\text{CD}_2} \approx 14$ kHz, i.e., the spectrum does not collapse to a single isotropic (so-called Lorentzian) line. So, we can conclude that n -butane in ZSM-5 is so confined that its motion is always ordered in some way and no isotropic reorientation is present. This qualitative result itself is interesting, but to make some more quantitative conclusions, which could be compared with available theoretical predictions,^{13,37,38} a further discussion about possible modes of n -butane dynamics is required.

While regarding intramolecular degrees of freedom, only torsional motions about the C–C bonds exhibit large angular displacements and thus can make a notable impact on the spectral line shape. These motions are the methyl group rotation and the conformational exchange. The latter is of major interest since it is highly sensitive to the confinement of the molecule

in the pores and could give some indications of the spatial distribution of the sorbate in the zeolite.^{13,37}

The mobility of the molecule as a whole is much more complex and can be described by hierarchical approach. For the motions of the smallest amplitudes, there exist librations and the “rocking motion”. Further, there are various uniaxial rotations^{13,14,39} or fast jump-exchange between different stable positions of *n*-butane in the inner space of the zeolite framework. One should take also into account, that since the geometry of the ZSM-5 channels and intersection is quite different,⁴⁰ the characteristics of these local motions at different places could be different. All these local motions are governed by weak dispersion interaction with walls of zeolite framework, and the experimental data show (vide supra) that they are characterized by the time $\tau \ll \tau_Q \approx Q_0^{-1} \approx 6 \times 10^{-6}$ s. On the largest scale of molecular motion one finds the diffusion: here the molecule reorientation occurs by fast jump exchange between different channels. As it was mentioned above the diffusion of *n*-butane in ZSM-5 was experimentally characterized by QENS,¹⁴ and reported residence times show that in our experimental range of temperatures the diffusion is also in the fast limit regime on the ^2H NMR time scale. This scale of molecular motion implies that within the characteristic time of NMR experiment ($\tau_Q \approx 10 \mu\text{s}$), the fast diffusing molecule performs all types of possible motions, exploring the whole volume of the zeolite channel-intersection system. This means that a molecule detailed dynamics report can be made only by MD simulation (a successful realization of such an approach can found in ref 17). As far as ^2H NMR line shape description is concerned, the correct line shape behavior can be described by more than one jump model. Therefore a simplified approach is required to characterize a variation of the line shape with temperature.

For such a problem the most adequate description method of the restricted molecular motion is based on the order parameter S , commonly used to characterize mobility of polymers, macromolecules, and liquid crystals.^{33,41} Within this approach we assume that *n*-butane (the CD_2 fragments) is involved only in fast conformational exchange so that the effective quadrupolar constant $Q_{\text{eff}} = S \times Q_1$, where S is the orientational (geometrical) order parameter which reflects how effectively the molecule averages the quadrupolar interaction, while exploring the inner volume of the zeolite pores. By definition, the S parameter includes the averaging effect of all non-intramolecular motions over whole pore volume. $Q_1 = f \times Q_0$ is the residual quadrupolar constant left after taking into account the internal motions, i.e., the trans/gauche isomerization (for CD_2 fragments). Here f is the averaging factor due to trans/gauche isomerization.

So from a formal point of view the overall motional averaging is expressed as $Q_{\text{eff}} = S \times f \times Q_0$. This formula reflects the hierarchical approach we have chosen, and its validity is based on certain physical assumptions: first of all, the concept of the order parameter in ^2H NMR spectroscopy can be applied only to a motion (or a set of motions), which are fast on the NMR time scale. As it was already discussed, this is our case. Since we define two distinct parameters, f for internal motions and S for the motions of *n*-butane as a whole, we need to assume that these two sets of motions can be considered as independent ones or, at least, that the hierarchy of characteristic times is preserved, i.e., the internal motions are faster than the motions of the molecule as a whole. The last condition is a less demanding one, and usually it is fulfilled at normal conditions but not at all temperatures: the common activation barriers for internal rotations in short alkanes are usually found in the range of 10–15 kJ mol $^{-1}$,⁴² while for diffusion QENS reports 5 kJ

mol $^{-1}$.¹⁴ So, it can happen, that at low temperatures the diffusion will actually be faster than the conformational exchange. However, we will show here that in certain cases the chosen approach is still valid. In fact, the direct simulation of the ^2H NMR spectra line shape shows that as far as a certain model is chosen with all motions in the fast limit regime, the final spectra line shape does not depend on the actual rate of each distinct motion. In other words, in the fast limit regime, the resulting Q_{eff} and η depend only on the chosen geometry of the motional model and not on the actual rates.³² In the pair of effective parameters of ^2H NMR spectrum, Q_{eff} and η , only η strongly depends on the order in the hierarchy. In most cases the effective interaction constant regards the molecular dynamics as a set of independent motions, while asymmetry parameter in contrary reflects how these motions are coupled.

Now, we can take advantage of the possibility to separate the internal motions and motions of *n*-butane as a whole: f depends on the relative populations of trans and gauche states, the higher the population of gauche conformation the less is f . $f = 1$, when $T \rightarrow 0$, and $f = 0.33$, when $T \rightarrow \infty$ and all conformers are equally populated. To be precise, when all conformations are equally populated, $f = (3 \cos^2 \theta - 1)/(2)$, in *n*-butane- d_{10} $\theta \approx 109^\circ$, which explains the mentioned number. Because of a difference in population of gauche conformers in a channel and at channel intersection¹³ f depends also on a molecule location in the zeolite framework. This gives the possibility to follow the distribution of *n*-butane in zeolite.

All together, the angle dependent effective quadrupole interaction frequency due to trans/gauche isomerization can be expressed by simple formulas (1–4). The static interaction tensor is characterized by $Q_0 \approx 170$ kHz and asymmetry parameter $\eta_0 \approx 0$, so each position of the C–D vector gives rise the static frequency

$$\omega^i(\theta, \varphi) = \sqrt{\frac{3}{2}} \frac{1}{2} \sum_{a=-2}^2 Q_0 D_{0a}(\Omega^i) D_{a0}(\varphi, \theta, 0) \quad (1)$$

Here i enumerates three conformers: trans, gauche+, and gauche–; $D_{ba}(\Omega^i)$ are usual Wigner rotation matrices,²⁶ which characterize the orientation of the C–D vector in each conformational position by a set of Euler angles Ω^i ; θ and φ are the polar angles which connect the molecular frame with the Zeeman (laboratory) frame. To get the averaged frequency we need to know the equilibria probabilities for trans/gauche conformations, which are expressed as $p_j^{\text{trans}} = (1)/(1 + 2 \exp(-(E_j)/(RT)))$ and $p_j^{\text{gauche}\pm} = (1 - p_j^{\text{trans}})/(2)$. The equilibria probabilities depend only on the temperature T and the energy difference E_j between trans and gauche states. The subscript j reflects the fact that in channels and intersections E are different,^{13,37} so there are 2 possible sets of equilibria probabilities.

In each position in the zeolites pore the averaging of the quadrupolar interaction by trans/gauche isomerization can be expressed as

$$\omega_j = p_j^{\text{trans}} \omega^{\text{trans}} + p_j^{\text{gauche}+} \omega^{\text{gauche}+} + p_j^{\text{gauche}-} \omega^{\text{gauche}-} \quad (2)$$

Because of the diffusion, there is a fast exchange between channel and intersection positions. Taking this into account we get the expression for the effective frequency

$$\omega_{Q_1} = \sum_j \rho_j \omega_j \quad (3)$$

where j runs two possible positions: molecules in channels (ch) and at intersections (int). ρ_j reflects the relative population of molecules in the channels and at channel intersections, respectively, and $\rho_{\text{ch}} + \rho_{\text{int}} = 1$.

Assuming a certain distribution (ρ_j) of n -butane in the zeolite and the energy difference between trans and gauche states (E_j) formulas (1–3) permit a direct estimation of the averaging factor f . Having this, the fitting of the experimental spectra can be done using the basic formula³²

$$\omega_{Q_{\text{eff}}}(\theta', \varphi') = \sqrt{\frac{3}{2}} \frac{1}{2} \sum_{a=-2}^2 q_{2a} D_{a0}(\varphi', \theta', 0) \quad (4)$$

$$q_{2a} = \left(-\frac{\eta}{2}, 0, \sqrt{\frac{3}{2}}, 0, -\frac{\eta}{2} \right) Q_{\text{eff}}$$

q_{2a} is the effective interaction tensor characterized by the effective asymmetry parameter η and effective interaction constant $Q_{\text{eff}} = S \times f \times Q_0$. θ, φ are the polar angles which connect the effective interaction tensor principal axis frame (i.e., the coordinate system where only diagonal elements of the interaction tensor have nonzero value²⁵) with the Zeeman frame.

The fitting was performed by a two steps procedure: first we fitted the experimental line shape by two static quadrupolar spectra to derive the effective interaction tensor parameters Q_{eff} , η , and then, we used the approach described above and separately regarded the trans/gauche isomerization and the order parameter S .

Figure 3 shows the effective interaction tensor parameters which allowed us to make almost perfect fit of the experimental spectral line shape (see column b of Figure 1). As expected, the Q_{eff} and η temperature dependences are quite pronounced and monotonous, except the last 4 temperatures. Within our simplified concept, the asymmetry parameter does not play any role since its accurate value depends on actual geometry of all motions and thus requires no special discussion. One other hand the η value has no special physical meaning in our case.

Thus the monotonous decrease of the interaction constant Q_{eff} could be explained by two temperature dependent factors: the order parameter S and the averaging by the trans/gauche isomerization of n -butane, which is reflected in a value f . The temperature dependence of trans/gauche isomerization needs additional discussion: a separate estimation of the energy difference barrier E_j is not possible in our case, since we can not isolate n -butane in a channel or at channel intersection to analyze its behavior. Thus the direct observation of the influence of pure conformational exchange on the spectra is not possible. However, E_j for channel and channel intersection can be estimated based on MD simulations performed by Theodorou et al.¹³ As a partial result of that work, the equilibrium probabilities for trans and gauche conformers in channels and at intersections at different temperatures and loadings were computed.¹³ Following those data we can estimate the free-energy differences $\Delta G_{\text{int}} \approx 2.4 \text{ kJ mol}^{-1}$ at the intersections (almost the same as in gas phase¹³) and in the channels $\Delta G_{\text{ch}} \approx 5.3 \text{ kJ mol}^{-1}$. At this point, to estimate the energy differences some knowledge or physically reasonable assumptions on the entropy differences (i.e., on the degeneracy of states) is required. In the present work, we have taken the assumption that the number of binding sites for trans conformers and gauche

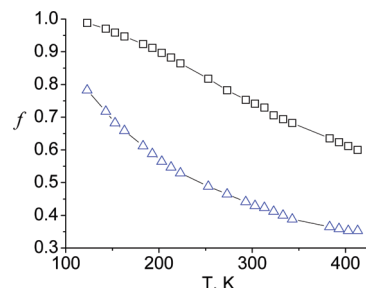


Figure 4. Temperature dependence of the averaging factor f of conformational exchange at two different positions within the zeolite framework: in the channel (\square , $E_{\text{ch}} = 5.3 \text{ kJ mol}^{-1}$) and at the intersection (Δ , $E_{\text{int}} = 2.4 \text{ kJ mol}^{-1}$).

conformers is equal. This statement requires justification: the zeolite ZSM-5 has 3 distinct sites: straight channels, zigzag channels, and intersections. Computations show⁴³ that the surface of its internal potential forms a rather smooth, slightly pressed cylinder or tube.⁴³ In such smooth and rather symmetric potential n -butane is restricted to have a single average position instead of multiple distinct, well-defined binding sites (of course it quickly rotates¹⁴ around this average position but makes our approximation even more efficient). Moreover MD simulations combined with neutron scattering measurements⁴⁴ have shown that small molecules like n -butane are much less sensitive to possible defects in the zeolite walls potential so that the diffusion coefficients for short alkanes are almost the same for zeolites with different density of structure defects. This proves, that the assumption that there is an equal number of positions for each conformer in the straight channel is a good one. For zigzag channels, the possibility for multiple binding sites looks higher. Fortunately, there is a direct experimental observation by TPD experiments,⁴⁵ which show that in terms of entropy there is only one adsorption site in ZSM-5 for n -butane. So in terms of entropy the straight and zigzag channels and all other possible binding sites for n -butane are equal. This means that we have an equal number of possibilities for each conformer in a zigzag channels and at the intersections. The question of adsorption sites in the intersections can also be regarded from a different point of view. It follows from the MD simulations¹³ the population of conformers at room temperature is very similar to the one measured for the gas phase. So, on one hand it is clear that even at the intersections n -butane is highly confined, but on the other one, the trans/gauche conformers seem to be not very sensitive to the inner potential of the intersections. In our opinion the assumption, that the degeneracy of the states in each location of n -butane inside the zeolite is equal for each trans/gauche conformer is a reasonable approximation. So we can estimate the energy differences as $E_{\text{int}} \approx 2.4 \text{ kJ mol}^{-1}$ and $E_{\text{ch}} \approx 5.3 \text{ kJ mol}^{-1}$.

Now we can use formulas (1–4) to simulate deuterium spectra. First, we separately treat the temperature dependent averaging by trans/gauche isomerization to see what difference one can get if places all molecules in channels or at intersections. The simulated temperature dependence of f for both positions are presented in Figure 4. As one can see, the conformational exchange averaging effect is considerably smaller in the channel (f is larger) than at the intersection. We find this result physically reasonable.

Having understood the possible influence of the internal motions due to trans/gauche isomerization on the quadrupolar constant we could finally fit the experimental data (see Figure 1). Figures 5 and 6 show the resulting simulation parameters, introduced above. The order parameter S is characterized by a

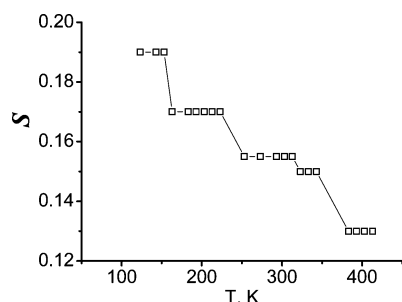


Figure 5. Temperature dependence of the order parameter S .

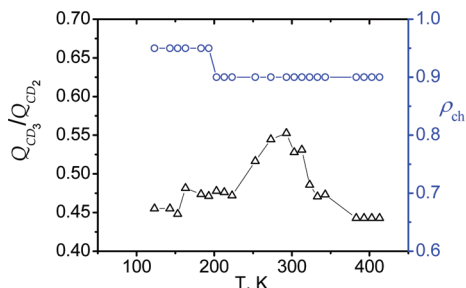


Figure 6. Temperature dependence of the relative population of *n*-butane molecules in the channels ρ_{ch} (O) and the ratio between Q constants for the CD_3 and CD_2 groups (Δ).

steplike temperature dependence. This can be rationalized by the following manner: the surface potential of the zeolites pore is not plain, and the effective accessible volume for a molecule depends on its average kinetic energy, i.e., on the temperature. The higher the temperature the less restricted is the motion of the adsorbed *n*-butane and the more efficiently the quadrupole constant is averaged. The fact that the temperature dependence is steplike means probably that there are a finite number of well-defined potential barriers on the inner surface of the zeolite channel walls which restricts additionally the molecule mobility.

Within the local temperature ranges where S is constant, a decrease of the constant Q_{eff} is purely due to decrease of f , i.e., due to increase of the population of gauche conformers. Since this increase of population is different for channels and channel intersections (see Figure 4), this property can be used to estimate the distribution of molecules within the zeolite pore system by eq 1. Figure 6 shows the result of the estimation: the major part of molecules resides inside the channels. This is in a good agreement with earlier theoretical results,^{13,37} where the preferred *n*-butane position in the channels of ZSM-5 was found to be energetically more favorable.

There is another interesting aspect of the spectra temperature behavior. At $T > 373$ K (see Figure 3) the line shape exhibits a sharp change: the constants Q_{eff} decrease to their lowest registered values and the asymmetry parameters drop to zero for both CD_3 and CD_2 groups (see Figures 1 and 3). Further, the line shape does not change anymore and the effective parameters remain unaffected by temperature increase. We suppose that above 373 K the volume of free space available for adsorbed molecules reaches its maximum and molecules are in the least possible ordered state. The zero value of the asymmetry parameters might imply that above 373 K one of the motions (not obligatory trans/gauche isomerization), in which the *n*-butane molecules are involved, transforms to a uniaxial rotation. Such hypothesis is supported by the study of *n*-butane mobility with QENS.¹⁴

The last observation to discuss is the ratio between Q_{eff} for the CD_3 and CD_2 groups. The temperature dependence of $Q_{\text{eff}}^{\text{CD}_3}/Q_{\text{eff}}^{\text{CD}_2}$

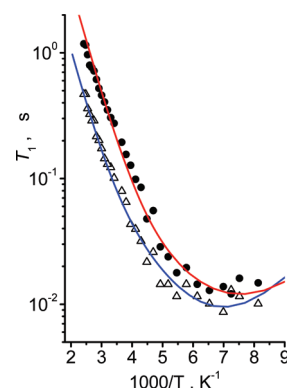


Figure 7. ^2H NMR spin-lattice relaxation times measured at perpendicular edges of powder patterns of the CD_2 (Δ) and CD_3 (\bullet) groups, together with simulation curves (solid lines) for *n*-butane- d_{10} adsorbed on H-ZSM-5 zeolite.

$Q_{\text{eff}}^{\text{CD}_2}$ is shown in Figure 6. The temperature variation of the ratio itself is not so remarkable, but the average value is. In fact the ratio is around ~ 0.5 at all temperatures, whereas it is expected to be around ~ 0.33 for immobile *n*-alkanes. In reality, such deviation of $Q_{\text{eff}}^{\text{CD}_3}/Q_{\text{eff}}^{\text{CD}_2}$ from 0.33 has no real physical meaning since it is not sufficient just to use the usual $(3 \cos^2 \theta - 1)/2$ factor with $\theta \approx 70.5^\circ$ (the supplement of the bond angle $\text{C}^2\text{--C}^1\text{--D}$, assuming the ideal tetrahedral of the methyl group) in order to take into account the methyl group rotation. Such approximation is valid only when all motions in which the molecule of *n*-alkane is involved, except the rotation of the methyl groups, are suppressed. If the rotation of the methyl group is additionally effected by the dynamics of another molecular fragment, one has to find a correct motional picture to obtain the effective interaction constant Q_{eff} . As it was already mentioned such a task is not possible without detailed MD simulations.

3.2. ^2H NMR Relaxation Data of Adsorbed *n*-Butane- d_{10} .

In the fast motional regime the deuterium spectra line shape provide no information on parameters of molecular dynamics other than the motional anisotropy: characteristic times and activation barriers could not be clarified. A measurement of the temperature dependence of spin-lattice relaxation time could be used to estimate them. Since the observed spectra manifest an anisotropic line shape, the relaxation time also exhibits a certain angular anisotropy, which represents an inconvenience in data analysis. To overcome this we measured the spin-lattice relaxation of both CD_2 and CD_3 groups only at the perpendicular edges of their spectra.⁴⁶ On the one hand the perpendicular edges are well-defined line shape features representing quadrupolar tensor orientations perpendicular to the magnetic field; on the other hand, it offers the best signal-to-noise ratio. The first point is also very important during the data analysis: since perpendicular edges indicate the exact angles which contribute to the chosen part of the spectrum (in fact, the main contribution to spin-lattice relaxation time at perpendicular edges of the spectrum come from $\theta = 90^\circ$), the anisotropy of the spin-lattice relaxation time can be correctly taken into account. The results, together with simulations are shown in Figure 7.

A trivial analysis based on a simple, model-independent approach shows that both experimental curves can be fitted by two $\sim \tau/(1 + \omega^2 \tau^2)$ terms with two distinct temperature dependent correlation times. In fact, both of the temperature dependence curves have two characteristic regions, with strongly different slopes: one from 123 K to approximately 173 K is almost flat (within the level of the experimental error), while the second

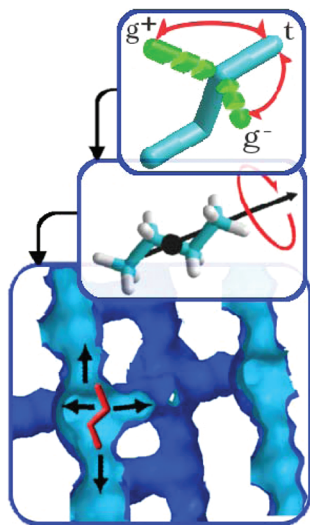


Figure 8. Schematic representation of the hierarchy of motions which affect the *n*-butane CD₂ groups ²H NMR spectra: on the internal level, *n*-butane is involved into conformation exchange, then the uniaxial rotation along the channel of the whole molecule (this motion is assumed to be fast even on the *T*₁ relaxation time scale), and on the largest scale *n*-butane is involved in translational diffusion via jump exchange between zeolite channels. The channels system fragment is taken from the Database of Zeolite Structures.⁴³

region from 173 to 413 K (the last experimental point) is characterized by a well pronounced and rather strong slope. The region with high slope indicates the presence of a motion with high activation energy (which can be estimated from the slope), while the broad “flat” region shows the presence of a motion with very small activation barrier. As usual the correlation times were assumed to follow the Arrhenius law $\tau_{1,2} = \tau_{1,2}^0 \exp(-E_{1,2}/RT)$.

A question arises, which dynamical modes correspond to these motions? Neutron scattering revealed translational diffusion and uniaxial rotation,¹⁴ while ²H NMR gives evidence for intramolecular conformational exchange and methyl group rotation. The spin–lattice relaxation is especially sensitive to motions with characteristic times $\tau_C \approx \omega_0^{-1} \approx (2\pi \times 61 \times 10^6)^{-1} \approx 10^{-8}–10^{-9}$ s, so the slope of the temperature dependence curve will depend mainly on the activation energy of a motion whose characteristic time is close to this value in the regarded temperature region. From QENS results we can estimate that *T*₁ should be governed mostly by diffusion in the low temperature region (so at 150 K, $\tau_D \approx 10^{-9}$ s). The uniaxial rotation is much faster; in fact this motion is well pronounced in neutron scattering experiments¹⁴ even at 120 K, which means that its correlation time $\tau_R \ll 10^{-9}$ s, i.e., it is probably the fastest motion in the system. So in the temperature range used in our study, the uniaxial rotation affects the spin–lattice relaxation time only as an averaging factor that decreases the effective interaction constant. From this, we can assume that the internal motions manifest themselves in the higher temperature region (see for example ref 23).

To simulate the relaxation times temperature dependence we have used the following model (schematically presented in Figure 8): the CD₂ group is involved in a 3-site conformational exchange, then free uniaxial rotation, and lastly a 4-site jump exchange of *n*-butane as a whole (i.e., its symmetry axis) among the channels. In the case of the CD₃ group, additional 3-site jump rotation was introduced. The resulting angle dependent spin–lattice relaxation time can be expressed by the following manner³¹

$$\frac{1}{T_1} = \frac{3}{4}\pi^2 Q_0^2 (J_1(\omega_0) + 4J_2(2\omega_0)) \quad (5)$$

where $J_m(\omega)$, the angle dependent spectral density function for the chosen model of the molecule motion is defined by the following expression^{31,47}

$$J_m(\omega) = 2 \sum_{a,a',b,b',c,c'=-2}^2 D_{m,a}(\Omega_L) D_{m,a'}(\Omega_L) C_{ab,a'b'}^D C_{bc,b'c'}^R C_{0c,0c'}^{\text{int}} \quad (6)$$

Here Ω_L are the observation angles θ and φ , which connect the crystalline frame (it is a frame attached to the zeolites unit cell, so that its *Z* axis is placed along the straight channel) with the laboratory frame; these angles define the angular dependence of the relaxation time, so since in our particular case we have chosen to follow the relaxation at a very specific position of the ²H NMR spectra (the perpendicular edges) these angles have certain fixed values. The $C_{ab,a'b'}(\omega)$ are the Fourier transform of the orientational correlation function $G_{ab,a'b'}(t)$ specific for each type of motion (we assume here that motions are independent, so each correlation function can be calculated separately)

$$G_{ab,a'b'}(t) = \langle D_{a,b}(\Omega, 0) D_{a',b'}(\Omega, t) \rangle \quad (7)$$

Function $C_{bc,b'c'}^R$ is a constant, and it is estimated from the effective interaction constant derived from the data fitting. Functions for diffusion ($C_{ab,a'b'}^D$) and conformational exchange ($C_{cc,e'e'}^{\text{int}}$) are evaluated in a way based on the jump model formalism^{31,47}

$$C_{ab,a'b'}(\omega) = \sum_{l,k,n=1}^N D_{a,b}^l(\Omega_l) D_{a',b'}^k(\Omega_k) A_{l,n} \left(\frac{-\lambda_n}{\lambda_n^2 + \omega^2} \right) A_{n,k}^{-1} \quad (8)$$

Ω_k are the Euler angles that connect the local reference (for the chosen type of motion) frame with the *k*th distinct position of the C–D bond within the assumed geometry of the jump model; $A_{l,n}$ is a matrix composed by eigen vectors of rate constant matrix *R* and λ_n are its eigen values; *R* is the rate matrix which is defined by the jump model. It is a square matrix by dimension of *N*, the total number of possible distinct jump positions (in our case *N* = 3 and *N* = 4, for conformational exchange and diffusion, respectively). By definition R_{ij} is the rate constant for the transition from configuration *j* to *i*. It must obey the following rules

$$R_{ii} = - \sum_{j \neq i} R_{ij}, R_{ij} p_{\text{eq}}(j) = R_{ji} p_{\text{eq}}(i) \quad (9)$$

The latter expression is simply the condition of microscopic reversibility. $p_{\text{eq}}(i)$ is the equilibrium population of the *i*th jump position. We assume that all channels are equivalent, while the temperature dependence of the population distribution of trans/gauche conformers was treated in the same way as in case of the spectra line shape fitting.

As it can be seen from Figure 7, our model gives a good fit of the experimental data. The simulation results are presented in Table 1. It follows from the fit that one of the two motions

TABLE 2: Parameters Used for Simulation of the ^2H NMR Spin–Lattice Relaxation Time–Temperature Dependence for *n*-Butane- d_{10} Adsorbed on H-ZSM-5 Zeolite^a

	Q_{eff} , kHz	E_{ci} , kJ mol ⁻¹	$\tau_{\text{ci}_0} \times 10^{12}$, s	E_{D} , kJ mol ⁻¹	$\tau_{\text{D}_0} \times 10^{11}$, s
CD ₂ groups	85	12	1.0	5	6
CD ₃ groups	85	11	0.5	5	6

^a Errors in estimating the parameters: $Q_{\text{eff}} \pm 8$ kHz; for activation barriers E_{ci} , $E_{\text{D}} \sim 10\%$; for all pre-exponential factors $\sim 40\%$.

has a activation energy of ~ 12 kJ mol⁻¹ and pre-exponential factor of $\sim 10^{-12}$ s, which are usual for trans/gauche isomerization and methyl group rotation.⁴² The second one has a relatively weak barrier of ~ 5 kJ mol⁻¹ and a pre-exponential factor of $\sim 10^{-11}$ s. This motion has parameters, which are very similar to the reorientation of a molecule due to the diffusion jumps between the zeolite channels.¹⁴

The parameters in Table 1 sustain our first rough approximation: the ^2H spin–lattice relaxation in *n*-butane- d_{10} is mainly governed by the internal conformational exchange and jump diffusion between channels. The derived parameters for trans/gauche isomerization are of typical values for *n*-butane.⁴² As for the translational jump diffusion, the activation energy is in good agreement with neutron scattering results,¹⁴ whereas the pre-exponential factor is about 2–3 times larger. This discrepancy is not significant and we believe that it is associated mainly with the relaxation times acquisition accuracy and the fact that a simplified model was used. The effective interaction constant $Q_{\text{eff}} \approx 85$ kHz, which is smaller than the expected 170 kHz for Q_0 . So the correlation function of the fast uniaxial rotation is reduced to a static factor $\sim 1/2$.

Conclusions

The combined analysis of deuterium NMR spectra line shape and spin–lattice relaxation time temperature dependences allowed us to make the following conclusions about *n*-butane behavior when confined by zeolite ZSM-5 pores at low loadings of 2 molecules per unit cell. In the experimental temperature range, adsorbed molecules are involved in fast (on ^2H NMR time scale) reorientations as a whole and intramolecular motions.

Intramolecular motions are represented by methyl group rotation and conformational exchange occurring at $\tau \approx 4\text{--}8 \times 10^{-11}$ s (at 300 K) with an activation barrier of $E_{\text{ci}} \approx 11\text{--}12$ kJ mol⁻¹. The equilibrium population of trans and gauche conformers is highly sensitive to the pore confinement and is notably different for the channel and the intersection sites. This allowed us to show that the distribution of *n*-butane in the zeolite framework is not uniform and molecules are located mostly in the channels.

The fast reorientation of the alkane molecule as a whole is a complex anisotropic motion which consists of jump exchange between neighboring channels, occurring at $\tau_{\text{D}} \approx 3.7 \times 10^{-10}$ s (300 K) with an activation barrier of $E_{\text{D}} \approx 5$ kJ mol⁻¹ and of other rotational modes that may correspond to uniaxial rotation and librations of *n*-butane in the pore. All these motions are coupled and in present investigation were treated within the order parameter *S* concept. *S* is a sterical factor, which reflects on how effectively the inner volume of the zeolites pore is explored by the adsorbed molecules. The nonzero value of the order parameter *S* shows that the free rotational reorientation of *n*-butane is completely suppressed within the zeolite framework reflecting the anisotropic nature of the translational motion. *S* factor drops down upon heating from 0.19 to 0.15 value. Such behavior

of *S* probably indicates that there are several well-defined potential barriers on the inner surface of the zeolite walls which additionally restrict the molecular mobility.

Acknowledgment. This work was performed in a frame of French-Russian Laboratory of Catalysis. The work was supported by the Russian Foundation for Basic Research (Grant Nos. 05-03-34762 and 09-03-93113).

References and Notes

- (1) Chang, C. D. *Catal. Rev. Sci. Eng.* **1983**, 25, 1.
- (2) Chen, N. Y.; Degnan, J., T. F.; Smith, C. M. *Molecular Transport and Reactions in Zeolites. Design and Application of Shape Selective Catalysts*; VCH Publishers, Inc.: Weinheim, 1994.
- (3) Yang, R. T. *Gas Separation in Adsorption Processes*; Butterworth Publishers: Stoneham, MA, 1987.
- (4) Karger, J.; Ruthven, D. M. *Diffusion in Zeolites and Other Microporous Solids*; Wiley-Interscience: New York, 1992.
- (5) Dwyer, J. *Nature (London)* **1989**, 339, 174.
- (6) Rols, S.; Jobic, H.; Schober, H. C. R. *Physique* **2007**, 8, 777.
- (7) Dubbeldam, D.; Calero, S.; Maesen, T. L. M.; Smit, B. *Phys. Rev. Lett.* **2003**, 90, 245901.
- (8) Bee, M. *Quasielastic neutron scattering*; Adam Hilger: Bristol, 1988.
- (9) Mezei, F. E. *Neutron Spin Echo*; Springer-Verlag: Berlin, 1979; Vol. 128.
- (10) Geil, B.; Isfort, O.; Boddenberg, B.; Favre, D. E.; Chmelka, B. F.; Fujara, F. *J. Chem. Phys.* **2002**, 116, 2184.
- (11) Theodorou, D. N.; Snurr, R. Q.; Bell, A. T. *Comprehensive Supramolecular Chemistry*, 1996; Vol. 7.
- (12) Auerbach, S. M. *Int. Rev. Phys. Chem.* **2000**, 19, 155.
- (13) June, R. L.; Bell, A. T.; Theodorou, D. N. *J. Phys. Chem.* **1992**, 96, 1051.
- (14) Jobic, H.; Bee, M.; Caro, J. In *Proceedings 9th International Zeolite Conference, Montreal, 1992*; von Ballmoos, R., Higgins, J. B., Treacy, M. M. J., Eds.; Butterworth-Heinemann: Boston, 1993; Vol. II, p 121.
- (15) Vasenkov, S.; Bohlmann, W.; Galvosas, P.; Geier, O.; Liu, H.; Karger, J. *J. Phys. Chem. B* **2001**, 105, 5922.
- (16) Zorine, V. E.; Magusin, P. C. M. M.; Santen, R. A. v. *J. Phys. Chem. B* **2004**, 108, 5600.
- (17) Saengsawang, O.; Schuring, A.; Remsungnen, T.; Loisuangsang, A.; Hannongbua, S.; Magusin, P. C. M. M.; Fritzsche, S. *J. Phys. Chem. C* **2008**, 112, 5922.
- (18) Schwartz, L. J.; Meirovitch, E.; Ripmeester, J. A.; Freed, J. H. *J. Phys. Chem.* **1983**, 87, 4453.
- (19) Stepanov, A. G.; Shubin, A. A.; Luzgin, M. V.; Jobic, H.; Tuel, A. *J. Phys. Chem. B* **1998**, 102, 10860.
- (20) Sato, T.; Kunimori, K.; Hayashi, S. *Phys. Chem. Chem. Phys.* **1999**, 1, 3839.
- (21) Boddenberg, B.; Burmeister, R. *Zeolites* **1988**, 8, 488.
- (22) Stepanov, A. G.; Alkaev, M. M.; Shubin, A. A. *J. Phys. Chem. B* **2000**, 104, 7677.
- (23) Kolokolov, D. I.; Arzumanov, S. S.; Stepanov, A. G.; Jobic, H. *J. Phys. Chem. C* **2007**, 111, 4393.
- (24) Kolokolov, D. I.; Glaznev, I. S.; Aristov, Y. I.; Stepanov, A. G.; Jobic, H. *J. Phys. Chem. C* **2008**, 112, 12853.
- (25) Abragam, A. *The Principles of Nuclear Magnetism*; Oxford University Press: Oxford, 1961.
- (26) Spiess, H. W. In *NMR Basic Principles and Progress*; Diehl, P., Fluck, E., Kosfeld, R., Eds.; Springer-Verlag: New York, 1978; Vol. 15, p 55.
- (27) Romannikov, V. N.; Mastikhin, V. M.; Hocevar, S.; Drzaj, B. *Zeolites* **1983**, 3, 311.
- (28) Powles, J. G.; Strange, J. H. *Proc. Phys. Soc.* **1963**, 82, 6.
- (29) Davis, J. H.; Jeffery, K. R.; Bloom, M.; Valic, M. I.; Higgs, T. P. *Chem. Phys. Lett.* **1976**, 42, 390.
- (30) Farrar, T. C.; Becker, E. D. *Pulse and Fourier Transform NMR. Introduction to Theory and Methods*; Academic Press: New York and London, 1971.

- (31) Wittebort, R. J.; Olejniczak, E. T.; Griffin, R. G. *J. Chem. Phys.* **1987**, *86*, 5411.
- (32) Macho, V.; Brombacher, L.; Spiess, H. W. *Appl. Magn. Reson.* **2001**, *20*, 405.
- (33) Jelinski, L. W. In *High Resolution NMR Spectroscopy of Synthetic Polymers in Bulk (Methods and Stereochemical Analysis)*; Komoroski, R. A., Ed.; VCH Publishers: New York, 1986; Vol. 7, p 335.
- (34) Schmider, J.; Muller, K. *J. Phys. Chem. A* **1998**, *102*, 1181.
- (35) Beck, B.; Villanueva-Garibay, J. A.; Muller, K.; Roduner, E. *Chem. Mater.* **2003**, *15*, 1739.
- (36) Stepanov, A. G.; Alkaev, M. M.; Shubin, A. A.; Luzgin, M. V.; Shegai, T. O.; Jobic, H. *J. Phys. Chem. B* **2002**, *106*, 10114.
- (37) June, R. L.; Bell, A. T.; Theodorou, D. N. *J. Phys. Chem.* **1990**, *94*, 1508.
- (38) Romanova, E. E.; Krause, C. B.; Stepanov, A. G.; Wilczok, U.; Schmidt, W.; van Baten, J. M.; Krishna, R.; Pampel, A.; Karger, J.; Freude, D. *Solid State Nucl. Magn. Reson.* **2008**, *33*, 65.
- (39) Maginn, E. J.; Bell, A. T.; Theodorou, D. N. *J. Phys. Chem.* **1995**, *99*, 2057.
- (40) Kokotailo, G. T.; Lawton, S. L.; Olson, D. H.; Meier, W. M. *Nature (London)* **1978**, *272*, 437.
- (41) Meirovitch, E.; Samulski, E. T.; Leed, A.; Scheraga, H. A.; Rananavare, S.; Nemethy, G.; Freed, J. H. *J. Phys. Chem.* **1987**, *91*, 4840.
- (42) Morrison, R. T.; Boyd, R. N. *Organic Chemistry*; Allyn & Bacon, Inc.: Boston, 1970.
- (43) Baerloche, C.; McCusker, L. B. Database of Zeolite Structures: <http://www.iza-structure.org/databases/>.
- (44) Feldhoff, A.; Caro, J.; Jobic, H.; Ollivier, J.; Krause, C. B.; Galvosas, P.; Karger, J. *ChemPhysChem* **2009**, *10*, 2429.
- (45) Millot, B.; Methivier, A.; Jobic, H. *J. Phys. Chem. B* **1998**, *102*, 3210.
- (46) Torchia, D. A.; Szabo, A. *J. Magn. Reson.* **1982**, *49*, 107.
- (47) Wittebort, R. J.; Szabo, A. *J. Chem. Phys.* **1978**, *69*, 1722.

JP908464F